Eur. Radiol. 10, 1487–1492 (2000)

Experimental radiology

European Radiology

Original article

Feasibility of synchrotron radiation computed tomography on rats bearing glioma after iodine or gadolinium injection

G. Le Duc[1], S. Corde[2], H. Elleaume[2], F. Estève[2], A.-M. Charvet[2], T. Brochard[1], S. Fiedler[1], A. Collomb[3], J.-F. Le Bas[2]
Jeune Equipe RSRM – UJF

[1] Medical Beamline, European Synchrotron Radiation Facility, BP220, Avenue des Martyrs, Polygone Scientifique, F-38043 Grenoble cedex, France
[2] Unité IRM, CHU, BP217, F-38043 Grenoble cedex, France
[3] Laboratoire de Cristallographie, CNRS, BP166, F-38043 Grenoble cedex, France

Received: 8 September 1999; Revised: 3 May 2000; Accepted: 4 May 2000

Abstract. The purpose of this work was to demonstrate the feasibility of a new imaging technique called synchrotron radiation computed tomography (SRCT). This technique leads to a direct assessment of the in vivo concentration of an iodine- or gadolinium-labeled compound. Rats bearing C6 glioma were imaged by MRI prior to the SRCT experiment. The SRCT experiments were performed after a 1.3 g I/kg ($n = 5$) or a 0.4 g Gd/kg ($n = 5$) injection. Finally, brains were sampled for histology. The SRCT images exhibited contrast enhancement at the tumor location. Ten minutes after injection, iodine and gadolinium tissular concentrations were equal to 0.80 ($\pm$ 0.40) mg/cm^3 and 0.50 ($\pm$ 0.10) mg/cm^3, respectively in the peripheral area of the tumor (respective background value: 0.20 $\pm$ 0.02 to 0.10 $\pm$ 0.01). Correlation to MRI and histology revealed that the contrast uptake occurred in the most vascularized area of the tumor. The present study summarizes the feasibility of in vivo SRCT to obtain quantitative information about iodine and gadolinium-labeled compounds. Beyond brain tumor pathology, the SRCT appears as a complementary approach to MRI and CT, for studying iodine- and gadolinium-labeled compounds by the direct achievement of the tissular concentration value in the tissue.

Key words: Synchrotron – Iodine – Gadolinium – CT – Brain – Glioma

Introduction

X-ray CT and MRI coupled to the injection of contrast agents are now common tools for 2D or 3D imaging of the human body. Current medical research is focused on the extension of the usefulness of these medical imaging techniques from anatomical mapping to functional and quantitative information such as cerebral blood volume (CBV) and its variations under physiological or pathological conditions [1, 2]. In the particular case of brain tumors, assessing quantitative parameters is a key issue to evaluate tumor growth. Nevertheless, it is difficult to quantify the local contrast agent concentration inside the body in CT as well as in MRI. Despite an excellent spatial and temporal resolution, CT scanner has known few developments in functional imaging due to the limits of X-ray tubes: source size; intensity variations; limited flux; and broad spectrum causing beam hardening, i.e., changes in the X-ray beam spectrum as it penetrates the patient, and diffuse scattering getting into the detector. In MRI, the effect of the contrast agent on the nuclear magnetic resonance signal is a complex function of the contrast agent characteristics (e.g., relaxivities, magnetic susceptibility, concentration, nature, size, biodistribution) as well as experimental parameters (e.g., magnetic field, echo time, repetition time). We propose in this study a new in vivo imaging technique called synchrotron radiation computed tomography (SRCT) as a complementary approach of MRI and CT to directly assess the contrast agent concentration inside the brain. Following previous feasibility results obtained from simulations and phantom experiments [3, 4, 5, 6, 7, 8, 9], in vivo experiments were carried out on rats bearing gliomas. The present study demonstrates the feasibility of in vivo SRCT studies and the ability to assess the absolute in vivo tissular concentration of iodine or gadolinium-labeled contrast agents.

Methods

Principle

Figure 1 shows the spectral distribution of the ESRF medical beamline X-ray source as compared with the flux available from a conventional X-ray source. Sever-

Correspondence to: G. Le Duc

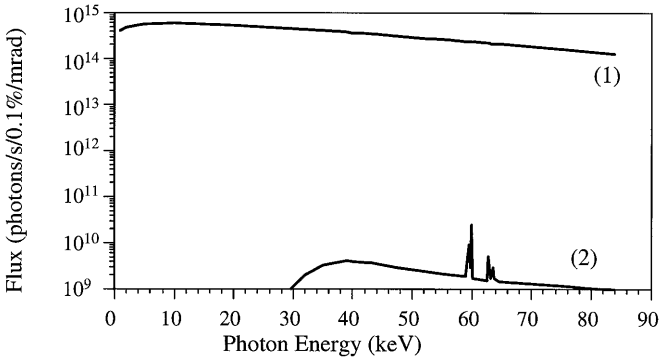

Fig. 1. Comparison between the spectral distribution of the beam available *1* from the ESRF medical beamline (ring current 200 mA, wiggler magnetic field 1.4 T, 1.6 m, 150 mm), and *2* from a conventional X-ray source (voltage 110 kV, filtered with 2.5-mm Al, 1 m from source)

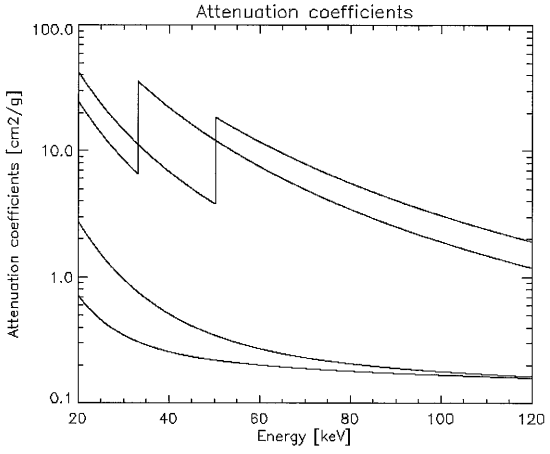

Fig. 2. Attenuation coefficient (cm^2/g) as a function of energy (keV) for **1** iodine, **2** gadolinium, **3** bone, and **4** soft tissues. K edges values are equal to 33.169 keV ($\Delta\mu/\varrho = 29.4\ cm^2/g$) and 50.239 keV ($\Delta\mu/\varrho = 14.73\ cm^2/g$) for iodine and gadolinium, respectively

al orders of magnitude separate the spectra in terms of flux. The high intensity and tunability of the source allow monochromatic beams to be generated by using a monochromator at any energy, enhancing the image contrast by selection of the most effective energy for a given procedure and suppressing beam artifacts. The SRCT experiments were performed by using a dual-energy subtraction technique. As shown in Fig. 2, this technique uses the sharp rise in the photoelectric component of the attenuation coefficient of iodine (or gadolinium) at the binding energy of the K electron. Two images obtained with monochromatic X-ray are simultaneously acquired, just below and above the K edge of the contrast agent. K edges values are equal to 33.169 keV ($\Delta\mu/\varrho = 29.4\ cm^2/g$) and 50.239 keV ($\Delta\mu/\varrho = 14.73\ cm^2/g$) for iodine and gadolinium, respectively. The resulting logarithmically subtracted image is quantitative for the contrast agent concentration in the sample since the bones and tissue contributions become negligible in the mathematical operation [6]. Such a concept has already been applied to angiography studies (intravenous coronarography) at the ESRF [10, 11].

Instrumentation

The set-up was first devoted to angiography experiments [10, 11] before being adapted to SRCT experiments both on phantoms and rats (Fig. 3). The monochromator is based on a single bent Laue silicon crystal [12], which creates two monochromatic beams characterized by a bandwidth equal to 200 eV in the case of both iodine and gadolinium. The two monochromatic beams (one above and one below the K edge separated by a splitter) are deflected upwards, at a mean angle of 6.84° at 33.169 keV and 4.51° at 50.239 keV according Bragg's law. They cross at the center of the sample and the two images are recorded simultaneously. The fan-shaped X-ray beam is 0.8 mm in height and 120 mm in width. Two translations (horizontal and vertical, respectively) are used for prepositioning of the sample and for multislice imaging. The acquisition is performed during a rotation of the sample of 360° around a vertical axis by means of a rotation stage. The attenuation is measured with a cryogenically cooled, high-purity germanium detector made with two rows of 432 pixels of 0.35 mm width each, and working in integration mode (Eurisys Mesure, Lingolsheim, France). The two lines allow to simultaneously measure X-ray transmission of the sample for both energies. The data acquisition electronics provide a very large dynamic range (16 bits). The timing to obtain one slice (i.e., to record 1440 projections) is approximately 24 s. It has to be stressed that this detector, specifically designed for human brain studies, was not optimized for rat brain studies. The cross-sectional images obtained from SRCT experiments are calculated from the numerous projections measured at small angular intervals. The data processing is performed under an IDL software called the SNARK code (University of Pennsylvania, Philadelphia). An in-house software allows the selection of regions of interest (ROI) of a given size in the image and then the measurement of the absolute tissular concentration of the contrast agent in milligrams per cubic centimeter after proper calibration [6].

Tumor model

The C6 glioma cell line was established by Benda et al. [13] from a methyl nitrosourea induced rat glioma. The experiments were carried out on ten female Wistar Wag rats weighing 180–200 g. The cell suspension (10^5 cells in 5 μl) was stereotactically injected in the right caudate nucleus of the rat brain (9 mm anterior to the interaural line, 3.5 mm lateral to the midline, 3.5 mm depth from the dura) [14] according to a method [15] derived from Kobayashi et al. [16]. Operatives procedures and animal care strictly conformed to the Guidelines of the French Government (decree no. 87–848 of 19 October 1987, license nos. 7593 and A38071).

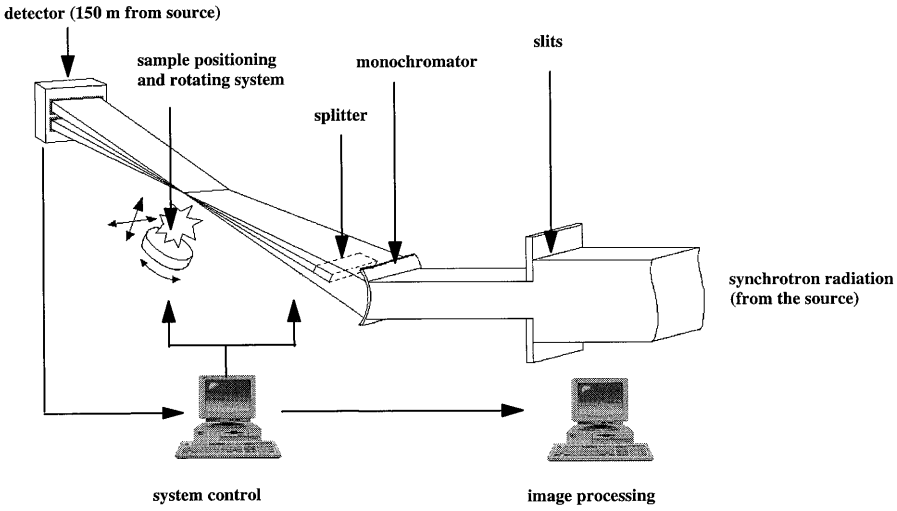

Fig. 3. Schematic view of the synchrotron radiation CT (SRCT) set-up

Imaging protocol

Prior to the SRCT protocol, glioma presence was checked by a conventional MRI examination (1.0-T Philips NT system, Philips, Best, The Netherlands) by using a T^1-weighted SE sequence (TR = 500 ms, TE = 20 ms, slice thickness 2 mm) coupled to a 0.15-mmol/kg gadolinium intravenous injection (Dotarem, Guerbet, Aulnay sous Bois, France). The SRCT images were acquired between 34 and 38 days after implantation of the tumor, i.e., at late tumoral stage. The same set-up was used for both iodine and gadolinium K-edge experiments, but not on the same series of rats since several hours are required to tune this energy from iodine to gadolinium K edge (two groups of five rats). The rats were anesthetized by means of an intraperitoneal injection (400 mg/kg of chloral hydrate) before placement in a vertical stereotactic holder screwed on the rotation motor. The contrast agents were injected in the saphena vein: iodine (Hexabrix, Guerbet, Aulnay sous Bois, France) was injected at 4 ml/kg (equivalent to 1.3 g I/kg), i.e., four times the clinical dose, whereas gadolinium (Dotarem, Guerbet, Aulnay sous Bois, France) was injected at 5 ml/kg (equivalent to 0.4 g Gd/kg), i.e., 25 times the MRI clinical dose. Four tubes filled with iodine or gadolinium were taped on the stereotactic frame close to the rat head as references for quantitative measurements. Contiguous multislice images 800 μm thick were acquired over a 12-mm height in order to scan the whole tumor. The time evolution of the contrast agent concentration was followed over 3 h at 10-min intervals after injection. For all experiments, the equivalent difference–image dose (skin-entry dose) was equal to 0.05 Gy/slice.

Histology

The animals were killed after the imaging experiments and the brains were excised, fixed in formalin and embedded in paraffin. Coronal sections of the tumor (3–5 μm) were obtained with a microtome and stained with hematoxylin and eosin (HE).

Results

For all rats bearing glioma in advanced stage, SRCT images taken either at the iodine (n = 5) or gadolinium (n = 5) K edge exhibit a contrast enhancement at the tumorlocation. Figure 4 shows a typical SRCT examination obtained on a rat brain bearing a glioma 10 min after iodine injection. After subtraction of the above and the below images, large vessels of the scalp and cheek muscles appeared hyperintense since they are opacified by iodine. The brain does not exhibit contrast enhancement except in the tumor area. Note that some elements do not disappear well in the subtraction (steel pin used as the reference for the centering of the reconstruction and stereotactic frame). Figure 5 shows images obtained on two rats bearing glioma after iodine and gadolinium injection, respectively. In both cases the tumor appeared heterogeneous with a well-delineated ring-shaped and hyperintense peripheral area, whereas the central part of the tumor exhibits a low enhancement. As shown in Table 1, the mean in milligrams per cubic centimeter (± SEM) was used to express the quantitative results obtained on each series of five rats in several ROIs. Highest tissular concentrations in the peripheral area of the tumor were measured to be 0.80 (± 0.40) mg/cm^3 and 0.50 (± 0.10) mg/cm^3 for I and Gd, respectively, whereas they were smaller in the center of the tumor: 0.60 (± 0.40) mg/cm^3 for iodine and 0.20 (± 0.20) mg/cm^3 for gadolinium. Values in the contralateral hemisphere of the brain were equal to 0.30 (± 0.10) and 0.10 (± 0.06) for iodine and gadolinium, respectively, i.e., close to background values (0.20 ± 0.02 for iodine and 0.10 ± 0.01 for gadolinium). The highest values were found in the muscles of the cheeks (1.80 ± 0.50 for iodine, 1.00 ± 0.30 for gadolinium).

Figure 6 highlights results obtained during a kinetic study at gadolinium K edge on a rat bearing a glioma. Image analysis as a function of time up to 2 h after injection showed that the peripheral hyperintense ring progressively expanded toward the center of the tumor. In others regions of the head (cheeks muscles as well as

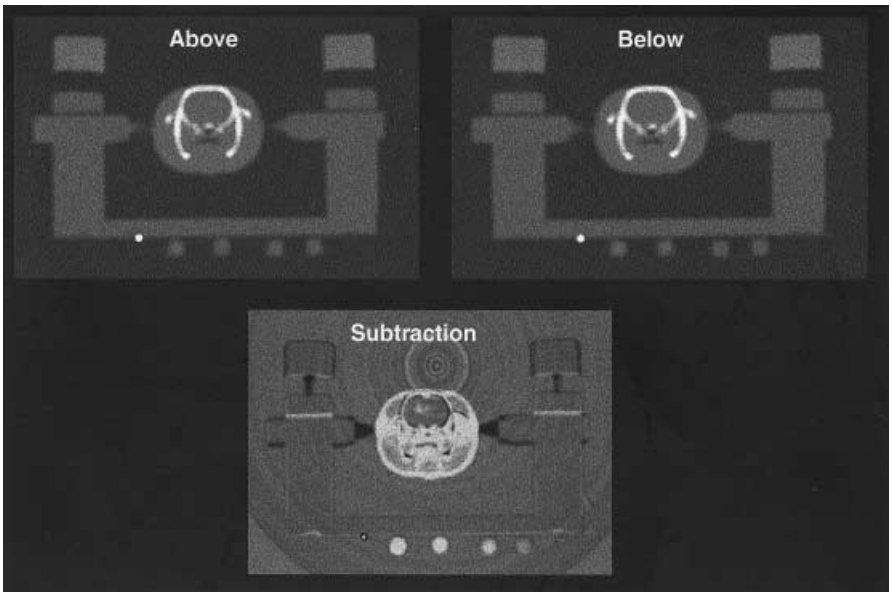

Fig. 4. An SRCT examination of a rat brain bearing a glioma obtained by logarithmic subtraction between images acquired above and below the iodine K edge, after intravenous injection of an iodine-based contrast agent (4 ml/kg). Note the contrast enhancement at the tumor location on the subtracted image and the presence of four reference tubes filled with several concentrations of iodine (from left to right: 2.5–1.25 – 1–0.5 g/cm^3)

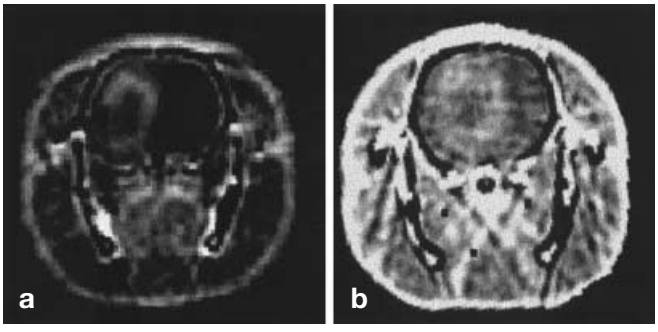

Fig. 5. Reconstructed SRCT image of a rat brain bearing a glioma obtained by logarithmic subtraction between images acquired above and below the K edge of **a** an iodine-based contrast agent (4 ml/kg), and **b** of a gadolinium-based contrast agent (5 ml/kg). The skin entry dose was equal to 0.05 Gy/slice

scalp) the signal progressively returned to the initial threshold. As shown in Fig. 7, the histological and MRI examination were undertaken to correlate SRCT images with standard techniques. For all rats, the contrast enhancement observed on the SRCT images was in good agreement with the MRI results and histological stainings. As an example, the Fig. 7 shows that the half-moon shape of the tumor is easily recognizable on both the MRI image and the histological staining. Moreover, the tumor exhibited typical glioblastoma features with a high vessel density in the peripheral part of the tumor.

Discussion

The images and quantitative data presented were obtained on five rats both at iodine and gadolinium K edge. Nevertheless, the accuracy of the measure is still critical. Improvements are on the way at several levels to optimize concentration measurements. The beam-crossing point must be evaluated with more accuracy for future experiments, leading to a complete disappearance of the stereotactic frame and bones in the subtraction. Reconstruction artifacts, such as ring artifacts (due to bad detector channels) and blunt-edge artifacts (due to sharp edges of the rat skull), must be removed since they create a background which affects our detectability threshold. In the same way, the reconstruction center must be chosen with more accuracy. Such improvements should lead to a better precision and are of great importance before starting data analysis on rat series, especially in the brain which is characterized by a CBV value close to 5 % [15]. Such improvements should also enable us to lower the injected quantities of contrast agents. This is of crucial importance in the case of gadolinium studies: gadolinium-based contrast agents are characterized by high relaxivity values at the expense of high concentration which was not the most important parameter for their efficiency in MRI. More concentrated contrast agents (typically five times) would be very helpful in this respect.

Nevertheless, the smallest distinguishable concentration reachable (corresponding to a signal-to-noise ratio of 3) is equal to 0.25 mg/cm^3 for iodine and 0.05 mg/cm^3 for gadolinium. The differences observed between io-

Table 1. Measured concentrations (n = 5, mean ± SEM) 10 min after injection of iodine and gadolinium in several regions of interest (ROI; skin entry dose: 0.05 Gy/slice). Iodine was injected at 4 ml/kg (equivalent to 1.3 g I/kg), whereas gadolinium was injected at 5 ml/kg (equivalent to 0.4 g Gd/kg)

	Measured value (mg/cm^3)	
ROI (size in pixels)	iodine image	gadolinium image
Periphery of tumor (13)	0.80 (± 0.40)	0.50 (± 0.10)
Center of tumor (2)	0.60 (± 0.40)	0.20 (± 0.20)
Contralateral (27)	0.30 (± 0.10)	0.10 (± 0.06)
Muscle (cheek) (13)	1.80 (± 0.50)	1.00 (± 0.30)
Phantom (79)	2.10 (± 0.2)	2.00 (± 0.02)
Background (2829)	0.20 (± 0.02)	0.10 (± 0.01)

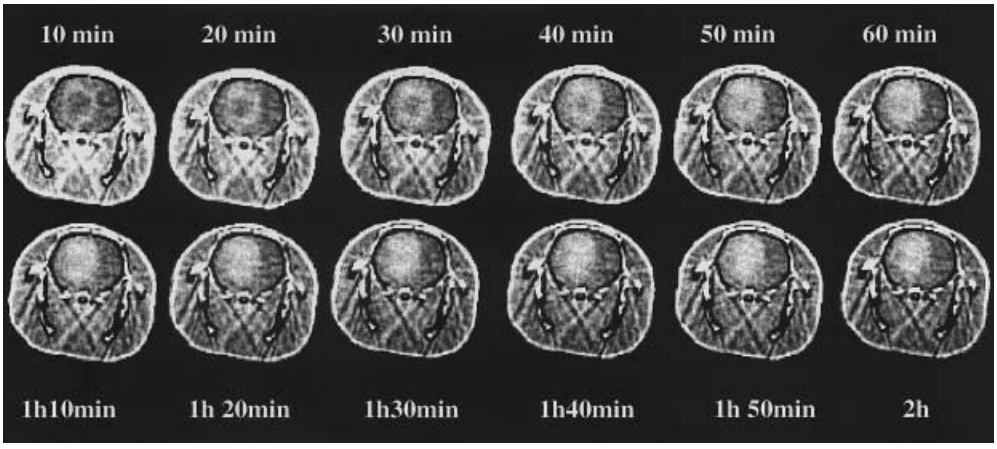

Fig. 6. Transverse SRCT images obtained every 10 min after a gadolinium-based contrast agent injection (5 ml/kg) on a rat brain bearing a glioma. The skin entry dose was equal to 0.05 Gy/slice

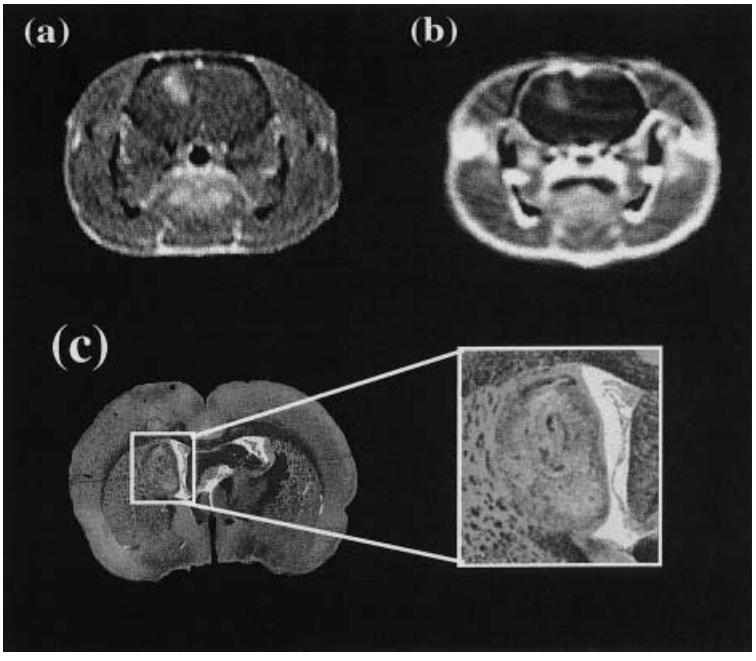

Fig. 7a–c. Transverse examination of a rat brain bearing a glioma. **a** An MRI image obtained with a T^1-weighted spin-echo sequence (TR = 500 ms, TE = 20 ms) after intravenous gadolinium injection. **b** An SRCT subtracted image obtained after intravenous iodine injection. **c** Hematoxylin and eosin staining. Note that the contrast enhancement visible both on MRI and SRCT images is fairly well correlated to the tumor shape and location

dine- and gadolinium-measured values for two same areas in the brain are due to the fact that the iodine solution was 3.3 times more concentrated than the gadolinium solution : 4 ml/kg or iodine are equivalent to 1.3 g I/kg, whereas 5 ml/kg of gadolinium are equivalent to 0.4 g Gd/kg. The measured values in the contralateral part of the brain (0.30 ± 0.10 for iodine and 0.10 ± 0.06 for gadolinium) are close to the background values (0.20 ± 0.02 for iodine and 0.10 ± 0.01 for gadolinium). Such small values in the contralateral brain could be explained as follows: (a) the blood volume is equal to 5 % of the total brain volume [17]; (b) the concentration of gadolinium chelates as well as iodine compounds in plasma decays to 30 % of the injected dose in 5 min [18, 19, 20]. In the tumor the peripheral part exhibits concentrations equal to 0.80 ($\pm$ 0.40) and 0.50 ($\pm$ 0.10) mg/cm^3, whereas the central part exhibits concentrations equal to 0.60 ($\pm$ 0.40) and 0.20 ($\pm$ 0.20) mg/cm^3 for iodine and gadolinium, respectively (Table 1). The peripheral hyperintense ring (corresponding to a strong attenuation) surrounding the tumor corresponds clearly on histological sections (Fig. 7) to a highly vascularized region. On the other hand, only few vessels were found in the central part of the tumor, characterized by necrosis features (Fig. 7). The ratio between the peripheral part and the central part of the tumor is equal to 1.33 for iodine and to 2.50 for gadolinium. This ratio is higher than previously obtained (1.25) on the same C6 model with a steady-state MRI CBV technique [21]. This discrepancy should be attributed to the fact that 10 min after injection, the gadolinium concentration measured is due mainly to the contribution of the blood-brain barrier (BBB) rupture component. On one hand, the contrast agent is washed out from the vessels due to a short blood half-life; on the other hand, the concentration inside the interstitial space increases, due to leakage of the contrast agent through the BBB rupture. The concentrations measured are signatures of both BBB phenomena and, to a lesser extent, CBV. Therefore, the kinetic study (Fig. 6) yields evidence of BBB rupture and

permeability to the contrast agent since the peripheral hyperintense ring (corresponding to a strong attenuation) progressively expands toward the central necrotic part of the tumor, whereas the contrast agent is washed out in the normal brain. These findings are clearly supported by the MRI examination which also yields evidence of BBB rupture (Fig. 7).

Conclusion

These preliminary results conclude the feasibility studies at the ESRF medical beamline. They illustrate the capabilities of the SRCT scanner prototype even if methodological improvements are essential. It is now possible to (a) obtain preclinical SRCT images with a 0.35-mm spatial resolution, i. e., close to MRI and conventional CT characteristics, (b) obtain a tissular concentration map of iodine- or gadolinium-labeled contrast agents in a living animal with a good correlation to phantoms used as references, and (c) correlate these images to conventional techniques such MRI and histology. On the basis of these results, K-edge SRCT will be used to study quantitatively angiogenesis and BBB rupture phenomena in the case of brain tumors, by carrying out both steady-state and first-pass experiments with several gadolinium-based contrast agents of different sizes. In this context the correlation of such results to MRI CBV techniques is of great importance.

In conclusion, the synchrotron source appears to be a very interesting tool for fundamental research on tumor knowledge and drug evaluation (labeled with iodine and gadolinium). Strong relationships with local research laboratories and with private companies involved in such programs are the keys to draft in parallel a protocol regarding human studies. Such protocols could be useful especially for the diagnosis and for the follow-up after therapy where a quantitative approach of angiogenesis and BBB rupture is an important goal. The SRCT technique does not aim at replacing conventional CT and MRI examination but could find applications in the field of neuropathology by helping to obtain quantitative information and to study gadolinium-based contrast agents (or drugs in general). Such a method should contribute to improve the art of diagnosis and contribute to improve basic knowledge of brain lesions and their evolution.

Acknowledgements. We thank all INSERM U438/U318, MRI staff, and Pathology Department of the CHU (Grenoble, France) for technical support and help, especially R. Farion. All experiments were made possible thanks to beamtime at the ESRF (Grenoble, France). Thanks also to the staff daily support (C. Nemoz and M. Rénier). This work was supported by Région Rhône-Alpes.

References

1. Rosen BR, Belliveau JW, Chen D (1994) Perfusion imaging by nuclear magnetic resonance. Magn Reson Imaging 5: 263
2. Hamberg LM, Kristjansen PE, Hunter GF, Wolf GL, Jain R (1994) Spatial heterogeneity in tumor perfusion with functional computed tomography at 0.05 microliter resolution. Cancer Res 54: 6032
3. Thompson AC, Llacer J, Campbell Finman L, Hughes EB, Otis JN, Wilson S, Zeman HD (1984) Computed tomography using synchrotron radiation. Nucl Instr Methods 222: 319
4. Dilmanian FA, Garrett RF, Thomlinson WC (1991) Multiple energy computed tomography for neuroadiology with monochromatic X-rays from the National Synchrotron Light Source. Nucl Instr Methods B56–57: 1208
5. Nachaliel E, Dilmanian FA, Garett RF, Thomlinson WC, Chapman LD, Gmur NF, Lazarz N, Moulin H, Rivers M, Rarback H, Stefan PM, Spanne P (1992) Monochromatic computed tomography of the brain using synchrotron X-rays: technical feasibility. Nucl Instr Methods 319: 305
6. Dilmanian FA, Wu XY, Parsons EC, Ren B, Kress J, Button TM, Chapman LD, Coderre JA, Giron F, Greenberg D, Krus DJ, Liang Z, Marcovivi S, Petersen MJ, Roque CT, Shleifer M, Slatkin DN, Thomlinson WC, Yamamoto K, Zhong Z (1997) Single and dual energy CT with monochromatic synchrotron X-rays. Phys Med Biol 42: 371
7. Le Bas JF, Charvet AM, Elleaume H, Bertrand B, Estève S, Spanne P, Suortti P (1995) Une nouvelle source de rayons X pour la recherche en imagerie médicale et en radiothérapie: le rayonnement synchrotron. Bull Cancer 82: 544
8. Elleaume H, Charvet AM, Le Bas JF (1997) The synchrotron beam, a new dimension for contrast media research? Acta Radiol 412: 29
9. Charvet AM, Le Bas JF, Elleaume H, Sculze C, Suortti P, Spanne P (1996) Medical applications of synchrotron radiation at the ESRF. In: Burattini E, Balerna A (eds) Proc Int School of Physics "Enrico Fermi" Course CXXVIII. IOS Press, Amsterdam, Netherlands, pp 355–377
10. Moulin H, Suortti P, Schulze C (1993) Angiography beamline at the ESRF. Phys Medica 9: 161
11. Elleaume H, Charvet AM, Berkvens P, Berruyer G, Brochard T, Dabin Y, Dominguez MC, Draperi A, Fiedler S, Goujon G, Le Duc G, Mattenet M, Nemoz C, Perez M, Rénier M, Schulze C, Spanne P, Suortti P, Thomlinson W, Estève F, Bertrand B, Le Bas JF (1999) Insrumentation of the ESRF medical imaging facility. Nucl Instr Methods A428: 513
12. Suortti P, Thomlinson W, Chapman D, Gmür N, Siddons D, Schulze C (1993) A single bent Laue monochromator for coronary angiography. Nucl Instr Methods A336: 304
13. Benda P, Someda K, Messer J, Sweet W (1971) Morphological and immunochemical studies of rat glial cells in tumors and clonal strains propagated in tissue culture. J Neurosurg 34: 310
14. Paxinos G, Watson C (1986) The rat brain in stereotaxic coordinates. Academic Press, New York
15. Benabid AL, Remy C, Chauvin C (1986) Experimental model of rat brain tumors by stereotactic injection of C6 glioma and HTC hepatoma cell lines. In: Walker MD, Thomas DGT (eds) Biology of brain tumors. Martinus Nijhoff, Amsterdam, Netherlands, pp 221–226
16. Kobayashi N, Allen N, Clendenon N, Nancy R, Ko LW (1980) An improved rat brain-tumor model. J Neurosurg 53: 808–815
17. Pawlik G, Rackl A, Bing RJ (1981) Quantitative capillary topography and blood flow in the cerebral cortex of cats: an in vivo microscopic study. Brain Res 208: 35–58
18. Allard A, Doucet D, Kien P, Bonnemain B, Caillé JM (1988) Experimental study of DOTA-gadolinium pharmacokinetics and phamacologic properties. Invest Radiol 23:S271–S274
19. Katzberg RW, Sahler LG, Duda SW, Morris TW, McKenna BA, Pabico RC, Niedrach WL, Tonetti FW (1990) Renal handling and physiologic effects of the paramagnetic contrast medium Gd-DOTA. Invest Radiol 25: 714–719
20. Weinmann HJ, Laniado N, Mützel W (1984) Pharmacokinetics of Gd-DTPA/dimeglumine after intravenous injection into healthy volunteers. Phys Chem Phys Med NMR 16: 167–172
21. Le Duc G, Péoc'h M, Rémy C, Charpy O, Muller RN, Le Bas JF, Décorps M (1999) Use of T2-weighted susceptibility contrast MRI for mapping the blood volume in the rat brain bearing a glioma. Magn Reson Med 42: 754–761